ISSN: 2710-0588

Collaborative Analysis of Vehicle Body and Battery Pack Structural Safety under Side Pole Impact Conditions

Qi Li, Min Li, Ke Wang, Yang Li

School of Mechanical and Automobile Engineering, Qingdao University of Technology, Qingdao, China

Abstract

To enhance the structural safety of pure electric vehicles under collision conditions, this paper constructs a finite element model of the entire vehicle side pillar collision that complies with the EURO NCAP regulations. A detailed analysis of structural safety during the collision process is conducted. The research focuses on key areas such as the B-pillar and the battery pack, quantifying the intrusion amount and acceleration variation characteristics by arranging spring elements and acceleration measurement points in the model. The results indicate that the acceleration peak at the corresponding position of the B-pillar chest is relatively high, posing a potential risk of occupant injury. The local intrusion amount of the battery pack exceeds mainstream design limits, reflecting a failure hazard in this area under extreme conditions. Coupled with the stress cloud map showcasing structurally weak regions, the primary reasons for the aforementioned hazard risks are further revealed to be insufficient strength of certain panels and limited energy absorption capacity. This paper proposes optimization suggestions such as reinforcement layout, material optimization, and structural energy absorption improvements, providing a theoretical basis and engineering reference for enhancing the collision safety of new energy vehicles.

Keywords

Battery Electric Vehicle; Side Pole Impact; Finite Element Analysis; Structural Safety; EURO NCAP.

1. Introduction

Due to the differences in power systems between pure electric vehicles and traditional fuel vehicles, their body structures also vary. During a collision, the battery pack, as one of the core components of pure electric vehicles, poses significantly higher safety risks than traditional models due to the presence of numerous battery cells and high-voltage components. Compared to fuel vehicles, the battery packs in pure electric vehicles are more susceptible to leakage and short-circuiting when subjected to impacts, which can lead to fire incidents that endanger passenger safety. Therefore, pure electric vehicles should not only focus on passenger safety but also pay close attention to changes in the structure of the battery pack [1-2].

Due to the highly nonlinear characteristics of the collision process, most scholars have established finite element models to simulate the changes in vehicle body under different collision conditions to assess vehicle safety performance [3]. In collision analysis, the acceleration and intrusion of key areas are widely regarded as core indicators for evaluating structural safety and occupant injury risk. Therefore, most studies focus on critical areas such as the front bulkhead, B-pillar, and steering wheel in the cockpit area, analyzing the variations in their acceleration and intrusion to evaluate the extent of injury sustained by occupants during a collision [4-6]. Currently, research on the structural safety of battery packs is quite diverse, including analyses of high-intensity load concentration conditions such as battery pack

ISSN: 2710-0588

crushing, scraping, and side pillar collisions [7-8]. Wang [9] et al. established a finite element simulation model for the battery pack under the scraping condition. By analyzing the deformation of the battery pack in the scraping condition, they proposed the installation of anti-collision rods and collision guiding brackets, effectively reducing the impact acceleration experienced by the battery pack by 40.7% and 52.9%, respectively. Yan [10] et al. evaluated the structural safety of the battery pack during a slight crushing process and revealed the deformation damage mechanism of the battery pack by analyzing its deformation and stress distribution.

Current research on vehicle collisions mainly focuses on the independent analysis of the vehicle body structure and battery pack, lacking systematic studies on the interaction between the body and battery pack during collisions. To address this gap, this paper constructs a finite element model for side pole collisions of the entire vehicle, with a particular emphasis on the collaborative response characteristics of the B-pillar and battery pack during the collision process. By analyzing the intrusion amounts, acceleration, and stress distribution at key locations, this study reveals structural safety issues present in this electric vehicle model and provides targeted optimization suggestions.

2. Model Construction and Validation of Effectiveness

2.1. Construction of Finite Element Model for Vehicle Side Pole Impact

The collision scenarios for complete vehicles generally include frontal collisions, 25% offset collisions, side collisions, and side pole collisions [11]. During frontal and 25% offset collisions, most of the energy generated is dissipated by the vehicle's front-end energy-absorbing space and energy-absorbing boxes. Additionally, compared to traditional side collisions, the impact loads generated during side pole collisions exhibit higher energy density and spatial concentration, posing a more significant threat to occupants, vehicle structure, vehicle power batteries, and intelligent control systems. Therefore, given the unique impact of side pole collisions on new energy vehicles, this paper primarily focuses on the research and analysis of side pole collision scenarios.

This paper sets up a model based on the requirements for side pillar collision conditions specified by the European New Car Assessment Programme (EURO NCAP). The vehicle collides with a rigid pillar of 254 mm in diameter at a speed of 29 km/h, with a collision angle of 90 degrees, and the collision point is aligned parallel to the Z-axis vertical line passing through the driver's center of mass. The side collision model is created using the Ls-Dyna solver under the HyperMesh software, with a total of 6,755,988 elements after mesh division. Among these, there are 4,330,061 quadrilateral QUAD4 elements and 242,190 triangular CTRIA3 elements, with triangular elements accounting for 3.5% of the total elements, meeting the model design requirements.

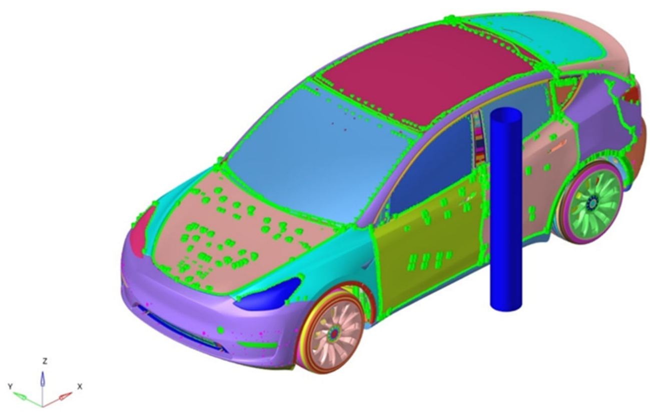

Figure 1. Finite Element Model for Vehicle Side Impact

ISSN: 2710-0588

2.2. Body deformation during collision process and effectiveness verification

After setting up the model according to the requirements for side pole impact conditions specified by the European New Car Assessment Programme (EURO NCAP), it was imported into the LS-DYNA solver for analysis. The simulation time was 0.12 seconds. The figure below illustrates the changes in posture of the entire vehicle and key components during the collision process.

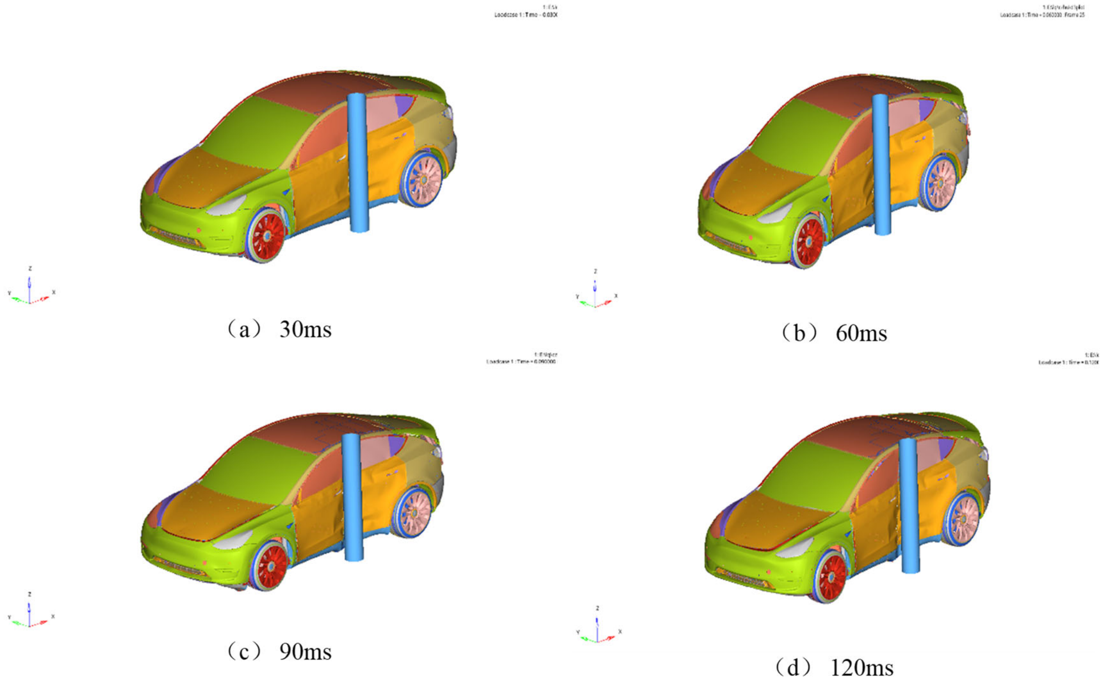

Figure 2. Whole Vehicle Collision Process Diagram

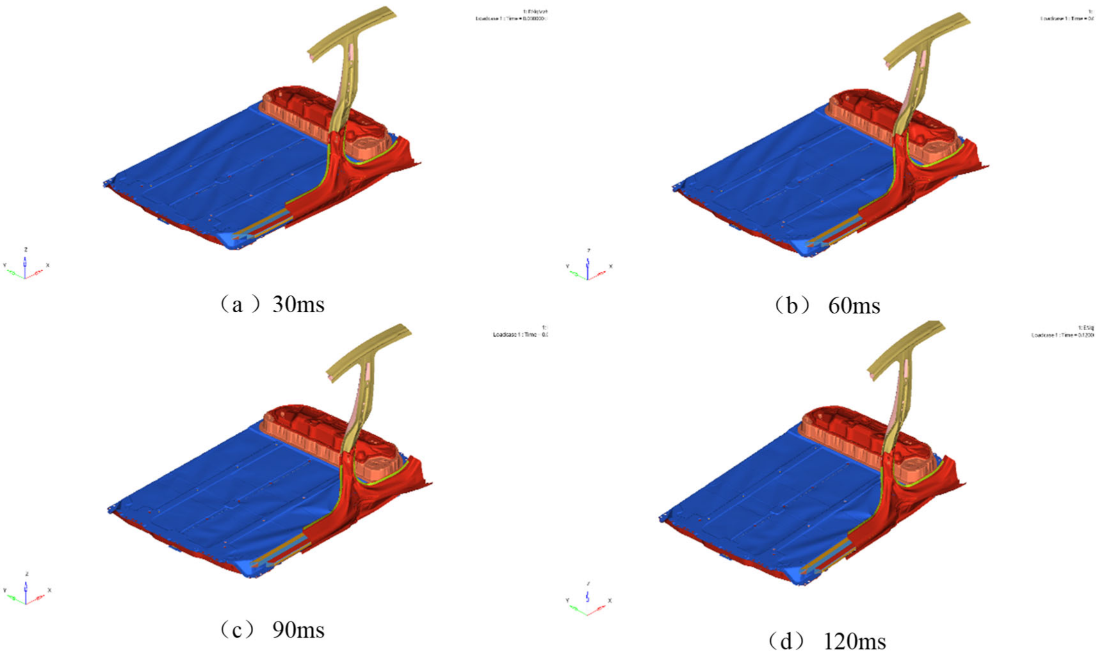

Figure 3. Diagram of the Collision Process at Critical Locations

ISSN: 2710-0588

To ensure the validity of the simulation process and results, this paper uses the changes in energy and mass as evaluation criteria. The energy change during the collision process primarily involves the conversion of kinetic energy into internal energy, thus it is essential to maintain the fundamental conservation of total energy. The sand clock energy serves as one of the critical indicators for assessing the stability and physical credibility of the calculations, and it must be ensured that the value of the sand clock energy ratio does not exceed 5%. Additionally, the ratio of the mass increase to the total mass should also be controlled within 5%.

Figure 4 illustrates the curves of energy and mass changes during the collision process. From the energy change curve, it can be observed that the vehicle makes contact with the rigid barrier at approximately 10 ms. As the collision progresses, the kinetic energy gradually decreases and is converted into internal energy. After 65 ms, the conversion between kinetic energy and internal energy stabilizes. Throughout the collision, the energy change curve exhibits a smooth trend, and the total energy of the system is essentially conserved. The ratio of sand clock energy to total energy reaches a maximum of 0.38%, which is significantly lower than the stipulated value of 5%. Regarding the mass change curve, the mass increased by 82 kg during the collision, which accounts for approximately 3.9% of the total mass, also well below the required 5%. Through the analysis of energy and mass during the collision process, it can be concluded that the established collision model is in basic alignment with actual conditions, and the data generated during the collision can be utilized for further in-depth research.

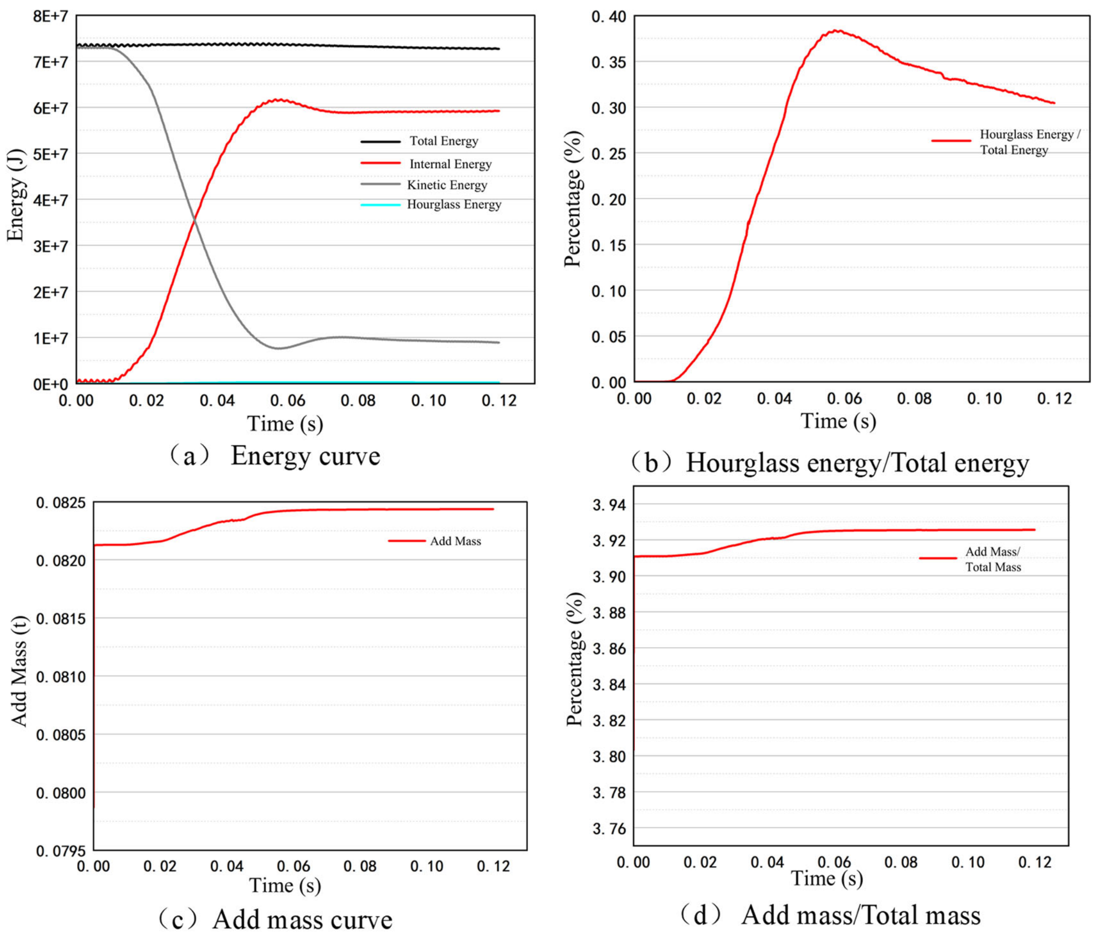

Figure 4. Energy Change and Mass Increase Curves

ISSN: 2710-0588

3. Analysis of Intrusion at Key Areas of Vehicle Body and Battery Pack

From the collision process diagram, it can be observed that the B-pillar of the vehicle and the battery pack casing exhibit significant deformation. The B-pillar is capable of dispersing and absorbing most of the impact force during the collision, thereby minimizing the risk of injury to the driver. Additionally, during the collision, the battery pack casing helps to reduce safety risks such as battery leakage and damage. By measuring the intrusion of the B-pillar and the battery pack casing, the intensity of the collision energy transmitted to the passenger compartment and the battery pack can be assessed, which allows for the prediction of potential impact injuries to the head, chest, and waist of the occupants, as well as to the battery cells and high-voltage lines within the battery pack. Therefore, the intrusion of the B-pillar and the battery pack casing during the collision process has a crucial impact on the safety of the battery pack and the life safety of the driver. This study sets up six spring elements between the B-pillars and the battery pack casing on both sides to evaluate their intrusion. Three of these are parallel to the driver's head, chest, and waist (Spring Element A, Spring Element B, Spring Element C), while the remaining three are evenly distributed along the Y-axis in the lower casing of the battery pack (Spring Element D, Spring Element E, Spring Element F), as illustrated in Figure 5.

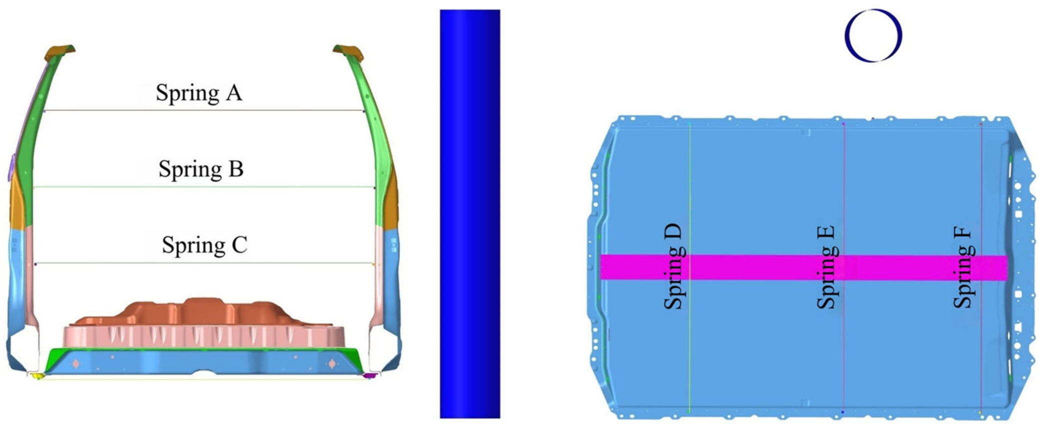

(a) Distribution positions of spring units in the B-pillar

（b）Distribution positions of spring units in the battery pack

Figure 5. Spring Unit Position Distribution

The positive value of the spring unit compression indicates compression in the positive Y-axis direction, while a negative value indicates stretching in the negative Y-axis direction. As shown in the figure, the B-pillar intrudes into the cabin due to compression caused by the impact. When the collision time reaches approximately 0.06 seconds, the intrusion reaches its peak value. The vehicle body gradually separates from the rigid column, and the B-pillar shows a tendency to rebound. The maximum intrusion occurs at the measurement position of spring unit B, with a result of 148.69 mm. According to the Euro NCAP collision standards, the inward displacement of the B-pillar during side column collision conditions should be controlled within a range of 150 mm to ensure occupant safety.

In contrast, the intrusion results at the three measurement locations on the battery pack lower shell exhibit relatively small fluctuations. The measurement points of Spring Unit E and Spring Unit F, being closer to the collision location, show an overall trend of compression in the positive direction along the Y-axis. Conversely, the measurement point of Spring Unit D, being farther from the collision position, is predominantly influenced by inertial factors, resulting in an overall trend of stretching in the negative direction along the Y-axis. According to the results

ISSN: 2710-0588

of the collision simulation analysis, the maximum intrusion occurs at the measurement point of Spring Unit E, with a peak displacement reaching 33.71 mm. Although the Euro NCAP collision test standards do not explicitly specify a limit for battery pack intrusion, mainstream automotive manufacturers generally adopt a design standard of maximum allowable intrusion for battery pack shells of ≤30 mm to ensure that the battery cells and high-voltage components are protected from mechanical damage. This study will further explore the key factors influencing battery pack intrusion based on this data.

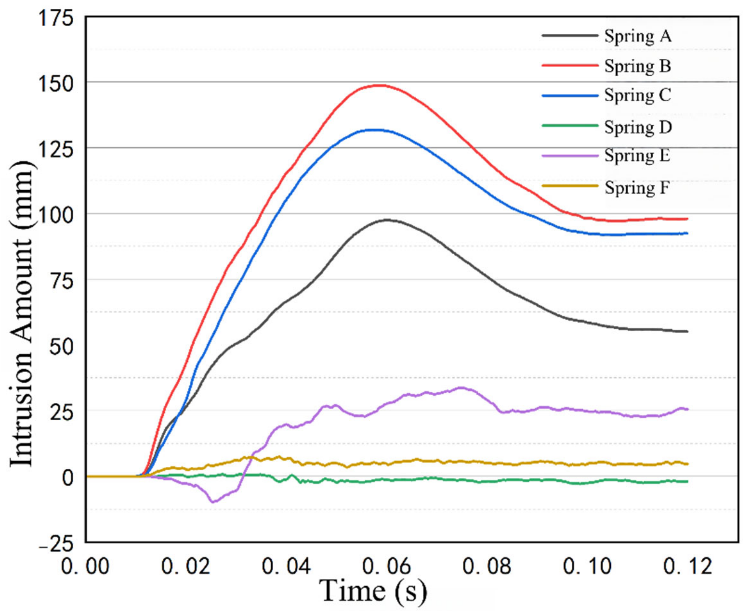

Figure 6. Intrusion Amount of B-Pillar and Sill Crossbeam

4. B-pillar and Battery Pack Acceleration Analysis

The acceleration of the B-pillar can reflect the energy absorption during a collision, aiding in the assessment of the potential impact on occupants and ensuring the integrity of the passenger compartment to protect the driver's safety. The acceleration data of the battery pack can assist in analyzing the forces acting on the battery pack during collisions or vibrations, and evaluating whether the battery pack has experienced impacts sufficient to trigger internal short circuits, thus ensuring its structural integrity and preventing internal short circuits or electrolyte leakage.

This study establishes two sets of acceleration measurement points. One set is located on the inner side of the B-pillar of the cockpit (measurement points A, B, and C), corresponding to the same height as the driver's head, chest, and waist. The other set is evenly distributed among the four battery packs within the battery module, with three measurement points set for each battery pack, totaling 12 measurement points (measurement points D to O). The specific distribution of these points is illustrated in Figure 7.

ISSN: 2710-0588

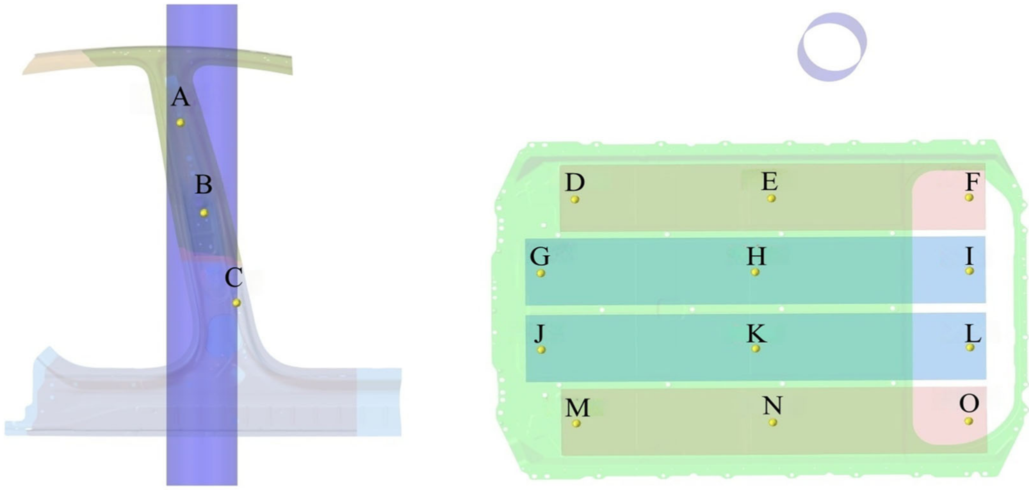

(a) B-pillar acceleration measurement point location
(b) Battery Pack Acceleration Measurement Point Location

Figure 7. Distribution Locations of Acceleration Measurement Points

As shown in Figure 8, the acceleration curve for the three measurement points on the B-pillar indicates that the peak values are primarily concentrated in the early stages of the collision, followed by a gradual stabilization of fluctuations. Notably, the acceleration peak at measurement point B is significantly higher than that of the other two measurement points, reaching a maximum of 164.1g, which corresponds to the driver's chest position. Although the Euro NCAP collision test standards do not specify a concrete limit for the acceleration of the B-pillar on the impact side, excessive acceleration implies that the absorbed impact load is reduced, leading to an excessive transfer of shock to the driver's chest, resulting in bruising and temporary chest discomfort.

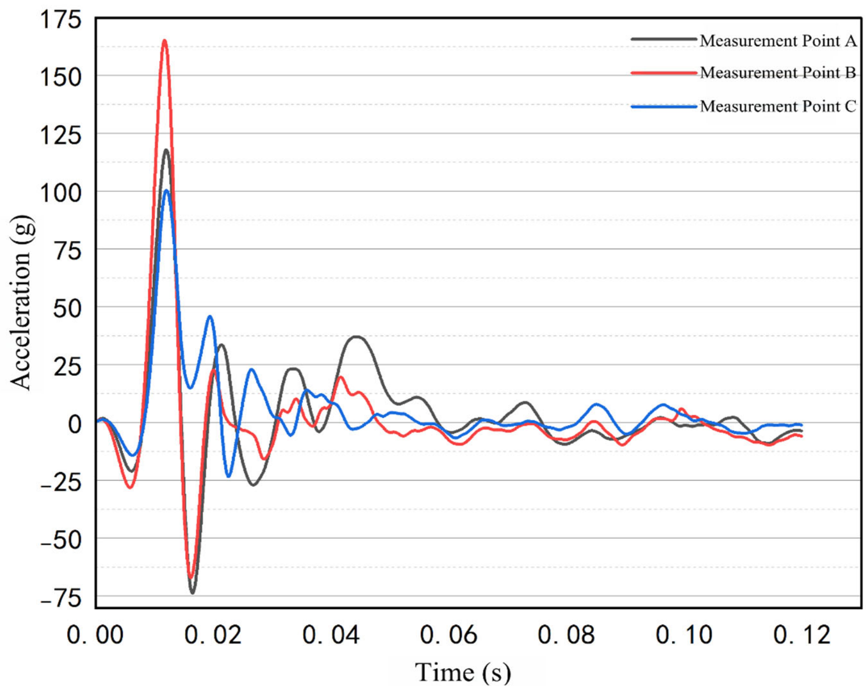

Figure 8. B-pillar acceleration

ISSN: 2710-0588

The peak acceleration of the battery packs is primarily concentrated during the entire process of contact between the vehicle and the side pillar, with three peak-valley regions occurring around 25 ms, 37 ms, and 50 ms. The peak acceleration of the first battery pack is recorded at measurement point F, yielding a result of 36.2 g; the peak acceleration of the second battery pack is observed at measurement point I, resulting in 37.1 g; the peak acceleration of the third battery pack is noted at measurement point L, yielding 36.8 g; and the peak acceleration of the fourth battery pack is recorded at measurement point O, resulting in 35.4 g. According to the Euro NCAP collision standards, the maximum acceleration of the battery pack should not exceed 50 g, thus all four battery pack acceleration values comply with the regulations.

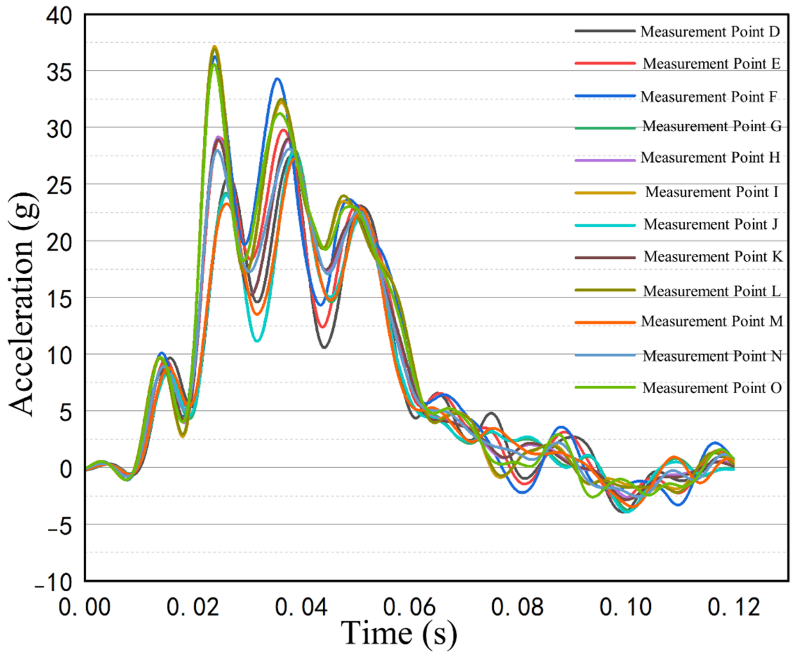

Figure 9. Battery Pack Acceleration

5. Stress Analysis of B-Pillar and Battery Pack

In the analysis of collision results, stress cloud maps of components can visually illustrate the stress distribution of various vehicle parts (such as the B-pillar, sill beam, battery pack, etc.) during a collision. In actual production and manufacturing, materials can be reinforced or structural designs optimized for components that experience stress concentration. This paper primarily considers the collision safety issues related to occupants and the battery pack; therefore, the battery pack and the B-pillar, which bears the main impact, are chosen as the subjects for stress analysis to identify areas of stress concentration and problematic components.

The stress distribution diagram reveals that there are three areas of stress concentration in the B-column: the top region of the B-column (approximately 1500 MPa), the mid-section reinforcement plate area (approximately 1000 MPa), and near the threshold beam (approximately 600 MPa). Based on the stress concentration, we can preliminarily infer that the excessive acceleration value at measurement point B is mainly due to two reasons: first, the upper protective plate at the top of the B-column undergoes plastic bending deformation, causing the impact force to be transmitted to the chest area, resulting in a sharp increase in acceleration; second, the mid-section reinforcement plate of the B-column lacks an effective energy absorption structure, preventing the impact energy generated from being dissipated effectively. To address the excessive acceleration issue, a gradient optimization of the material density distribution of the upper protective plate of the B-column can be performed, and a honeycomb buffer structure can be introduced within the B-column's reinforcement plate.

The stress concentration areas of the battery pack are mainly distributed along the edges of the upper shell. The stress peak at the collision side edge reaches 406.3 MPa, significantly exceeding the yield strength of the aluminum alloy 6061-T6 at this location (276 MPa). The maximum stress value far surpasses the yield limit of the material, resulting in noticeable wrinkling of the upper shell. This location corresponds to the stress concentration area of the aforementioned threshold beam, indicating that the transmission path of the impact force primarily goes from the threshold beam to the edge of the battery pack upper shell. Based on this analysis, it can be preliminarily inferred that the excessive intrusion at measurement point E of the battery pack is due to insufficient strength of the stress concentration areas between the threshold beam and the upper shell of the battery pack. After being subjected to forces, the two parts undergo cooperative deformation, leading to excessive intrusion. To address this issue, the following optimization measures can be taken: reinforcing ribs can be added inside the threshold beam to enhance local load-bearing capacity, and reinforcement components can be placed at the edge of the battery pack upper shell to improve its resistance to deformation.

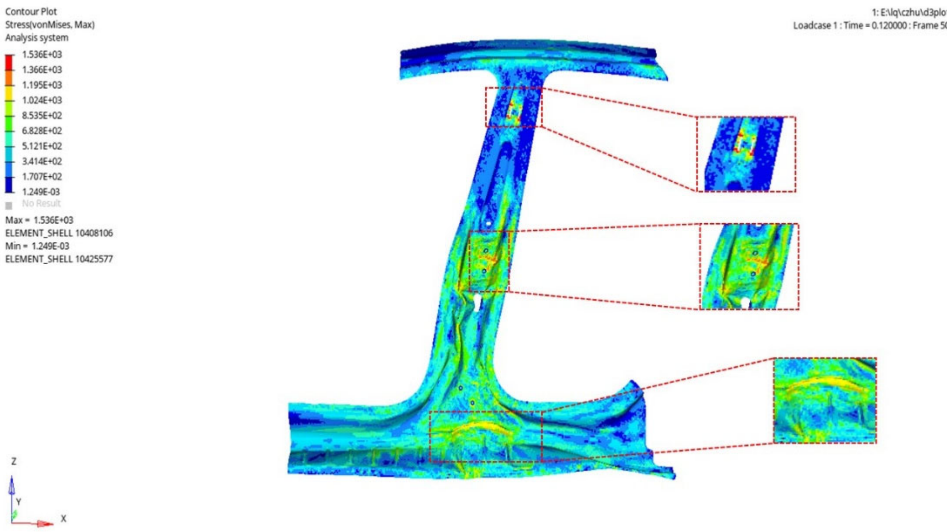

Figure 10. Stress Distribution Diagram of B-Pillar Panel

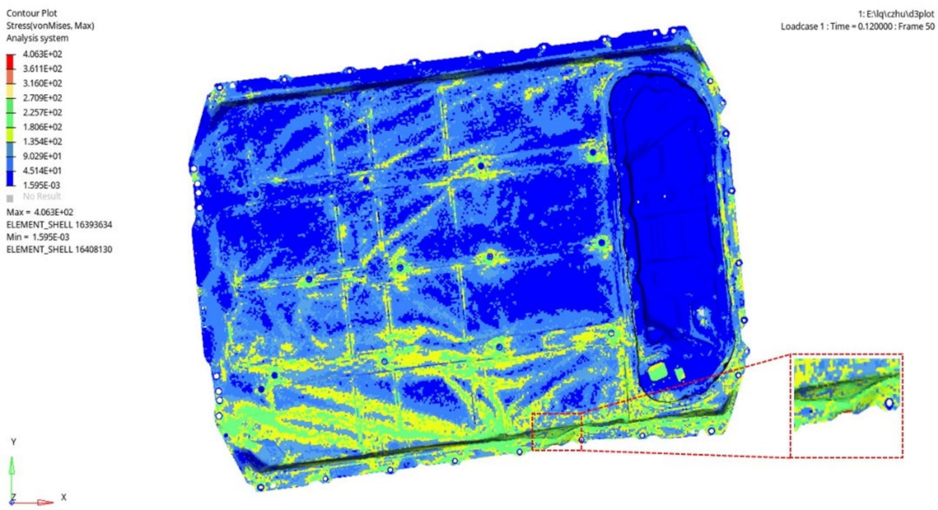

Figure 11. Stress Distribution Diagram of the Battery Pack

ISSN: 2710-0588

6. Conclusion

This paper establishes a finite element model for the side pillar collision of a certain electric vehicle using the Ls-Dyna solver under HyperMesh software, and conducts an in-depth analysis of the safety performance of key components under this collision scenario, mainly including the intrusion amount, acceleration, and stress distribution of the B-pillar and battery pack:

1) By arranging spring elements at critical locations of the B-pillar and battery pack, the dynamic changes in the intrusion amount of various components during the collision process were quantified. The results show that the maximum intrusion of the B-pillar is 148.69 mm, which basically meets the Euro NCAP standards, while the maximum intrusion of the battery pack reaches 33.71 mm, slightly exceeding the 30 mm limit set by mainstream automotive companies.

2) By setting up accelerometers inside the B-pillar and the four battery packs, the analysis of the acceleration results indicates that the peak acceleration at the measurement point corresponding to the driver's chest reaches 164.1g, suggesting insufficient structural energy absorption, while the acceleration of the battery pack is maintained below 50g, in compliance with safety regulations.

3) Stress analysis further reveals that the top area of the B-pillar, the middle reinforcement plate area, the threshold beam area, and the edge of the battery pack casing are the main high-stress concentration areas. Combined with the characteristics of stress distribution, the key influencing factors leading to excessive intrusion and abnormal acceleration are clarified, providing specific directions for structural optimization and design basis for subsequent improvements.

References

[1] Nan Chen, Bingbing Li. “Research progress on structural design and analysis of power battery packs for electric vehicles”, Machinery Manufacturing & Automation, Vol. 51, No. 1, pp. 1-6+10, 2022.

[2] Yufei Liu, Zhijun Wu. “Safety analysis of battery pack structure in pure electric vehicles”, China Science and Technology Information, No. 20, pp. 126-129, 2024.

[3] Ning Jia, Xingchao Wang, Keqi Wu, et al. “Nonlinear theoretical calculation method for automobile–w-beam guardrail collisions”, China Journal of Highway and Transport, Vol. 38, No. 3, pp. 200-210, 2025.

[4] Pengshan Xu. “Crashworthiness analysis of vehicles after 40% frontal overlap crash and body repair”, Machinery Research & Application, Vol. 38, No. 1, pp. 180-183, 2025.

[5] Lanlan Liu, Lei Qiu. “Lightweight design analysis of automobile B-pillar based on side impact safety”, Machinery Design & Manufacture, No. 4, pp. 283-286+293, 2025.

[6] Xinghua Wang, Lin Hu, Yong Peng, et al. “Driver risk perception in car–motorcycle collisions”, Automotive Engineering, Vol. 46, No. 3, pp. 498-508, 2024.

[7] Chenghao Ma, Zongxuan Shen, Jun Wang, et al. “Rapid prediction of battery pack crash safety in side pole impact conditions”, Automotive Engineering, Vol. 47, No. 1, pp. 117-126, 2025.

[8] Xin Lu, Jiaqi Wang, Liduo Chen. “Protective design of battery pack bottom under underfloor scraping conditions”, Battery Industry, pp. 1-11, Online First, 2025-07-27.

[9] Guojie Wang, Hailong Yu, Enze He, et al. “Design of electric vehicle frontal underfloor scraping condition and optimization analysis of battery pack protection”, Journal of Automotive Engineering, Vol. 12, No. 3, pp. 294-300, 2022.

[10] Pengfei Yan, Tianyi Ma, Guanglei Zhao, et al. “Simulation analysis of electric vehicle battery crush damage based on LS-DYNA”, Electromechanical Engineering Technology, Vol. 52, No. 6, pp. 139-142, 2023.

ISSN: 2710-0588

[11] Shunan Zhang. “Optimization research on vehicle crash safety considering body vibration”, Master Thesis, Qingdao University of Technology, 2024.